

Classification of seismic facies using seismic multi-attribute

Nelia Cantanhede Reis¹, Luiz Fernando Santos¹, Mayara Gomes Silva¹, Marcelo Gattass¹, Carlos Rodriguez¹

¹*Tecgraf Institute, Pontifical Catholic University of Rio de Janeiro - PUC-Rio
Prédio Pe. Laércio Dias de Moura, R. Marques de São Vicente, 255 Gávea, 22451-900, Rio de Janeiro/RJ, Brazil
neliareis@tecgraf.puc-rio.br; lsantos@tecgraf.puc-rio.br; mayaragomes@tecgraf.puc-rio.br;
mgattass@tecgraf.puc-rio.br; carlosrodriguez@tecgraf.puc-rio.br*

Abstract. Seismic interpretation is a fundamental process for hydrocarbon exploration. This activity consists of identifying geological information through the processing and analysis of seismic data. With seismic data's rapid growth and complexity, manual seismic facies analysis has become a significant challenge. Mapping seismic facies is a time-consuming process that requires specialized professionals. The objective of this work aims to apply multiattribute classification using a deconvolution neural network to map the seismic facies and assist in the interpretation process. We calculate a set of seismic attributes using Opendtect version 6.6 software from the amplitude data contained in the Facies-Mark Dataset. They are: Energy, Pseudo Relief, Instantaneous Phase, and Texture, all selected by an interpreter. The results showed that the attributes obtained a satisfactory result, reaching 85.15%, and the attributes together with the amplitude obtained 85.73%, while the amplitude, which is the most commonly used data in seismic classification, obtained 81.23%, based on the FWIU metric. In a direct comparison between the model with data augmentation and with attributes, the second performed better.

Keywords: Seismic attributes, Facies seismic, Neural networks, Classification

1 Introduction

In the context of hydrocarbon exploration, the most used geophysical tool is the seismic reflection method, which uses the principles of seismology to estimate the properties of the Earth's subsurface based on the reflection of seismic waves. After acquisition and processing, we reach the seismic data interpretation stage, which will obtain the most detailed information about the approximate location of the study of petroleum equipment for further exploration [1].

Seismic interpretation is one of the essential procedures in locating hydrocarbons. In the area of oil exploration, lithological discrimination becomes an essential task since it describes the physical characteristics of rocks and their respective layers. Based on this description and knowing the location of each type of rock, it is possible to infer where the formations that generate hydrocarbon concentration and, mainly, reservoirs. From the data analysis, specialists can identify structural and stratigraphic features. However, seismic interpretation and analysis is an arduous and time-consuming task that can overwhelm interpreters as the amount of geophysical information continually increases [2].

Seismic attributes emerged in an attempt to transform the seismic interpretation process from something less subjective and experience-based, into a faster and more objective process, mainly when working with volumes of 3D seismic data. They are an excellent data analysis tool that complements the interpreter experience by automatically highlighting, identifying, and correlating seismic data events with actual geological structures [3].

This work presents a methodology for automatically classifying seismic facies using seismic multi-attribute. The advantage of a multi-attribute classification is to integrate multiple information in a single classification process, and thus provide an integrated result containing the best information each one can offer.

2 Related Works

Liu et al. [4] proposed using two networks for seismic facies classification; one was a convolutional neural network (CNN) and the other an adversarial network (GAN). They performed three tests, the first with the supervised CNN using labeled synthetic data, the second with the semi-supervised GAN using synthetic CNN data,

only a few labeled samples, and finally, the semi-supervised GAN on the F3 seismic data of the Dutch sector of the North Sea. The best result was for GAN, compared to CNN, using little labeled data, which showed that this strategy is quite sound when we do not have a large amount of annotated data.

Alaudah et al. [5] proposed a deconvolution network architecture to classify seismic facies. The work compares the model in two strategies: with the use of patches and the other based on the entire seismic section. In addition, they used data augmentation techniques and skip connections. The best result found was the section-based model using augmentation and skip connections.

In Li et al. [6] they proposed a deep dilatation convolutional neural network based on trainable soft attention mechanism (ADDCNN) to improve the automatic analysis of seismic facies. The proposed ADDCNN model includes three main innovative frameworks: feature engineering, dilated convolutions, and spatial-spectral attention mapping. They used the F3 Block data to carry out the experiments, an independent expert labeled the Dataset samples, the intersection over union (IoU) was adopted as the evaluation metric. The results were compared with other networks in the literature with the same objective, the ADDCNN proved to be very efficient and surpassing the opponents.

El Zini et al. [7] implemented SeisNet, a convolutional neural network with a “butterfly” architecture that overcame the limited data challenge by implementing Data Augmentation and Transfer Learning techniques. Initially they used the network to detect bright spots in seismic data. Then they tested the same network for classification of seismic facies, in both experiments the results were satisfactory.

Zhang et al. [8] built a 3D CNN and another with an encoder-decoder architecture, then applied an improved encoder-decoder. They made use of data augmentation in an automatic and diversified way, using labeled 2D seismic sections in which the facies are divided into nine classes. They performed experiments on the Netherlands F3 dataset. The encoder-decoder test results were more accurate and efficient than those of CNN. The average values of intersection over union (IoU) for encoders-decoders were 87.8% (conventional) and 92.4% (enhanced), respectively, while for CNN, the value was 67.8% .

3 Methodology

This section describes the steps we take in developing the work. Figure 1 presents, in summary, the sequence of steps used in this work.

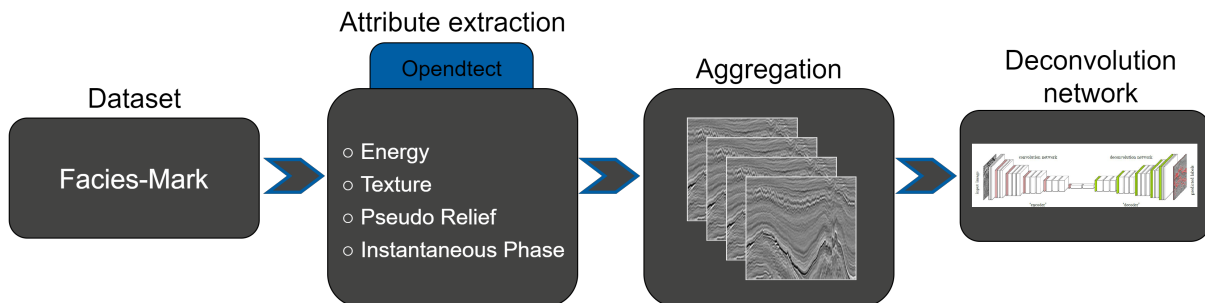


Figure 1. Proposed methodology

3.1 Dataset

To evaluate the methodology of this work, the Facies-Mark Dataset generated from the F3 Block by [5] was used. The authors created a 3D geological model of the F3 block, using well logs and 3D seismic data. Within this geological model, they identified seven groups of lithostratigraphic units, namely: High North Sea, Middle North Sea, Lower North Sea, Chalk, Rijnland, Scruff, and finally the Zechstein. However, the authors ended up unifying the Rijnland and Chalk classes, because they found it difficult to define a threshold between them. Thus, each of the six classes represents a seismic facies. Figure 2 shows an inline and its respective label; both data samples are part of the Dataset. The Dataset is quite unbalanced, as shown in Table 1 it contains the names of each class and their corresponding colors shown in Figure 2(b), as well as their percentages of pixels in the training set.

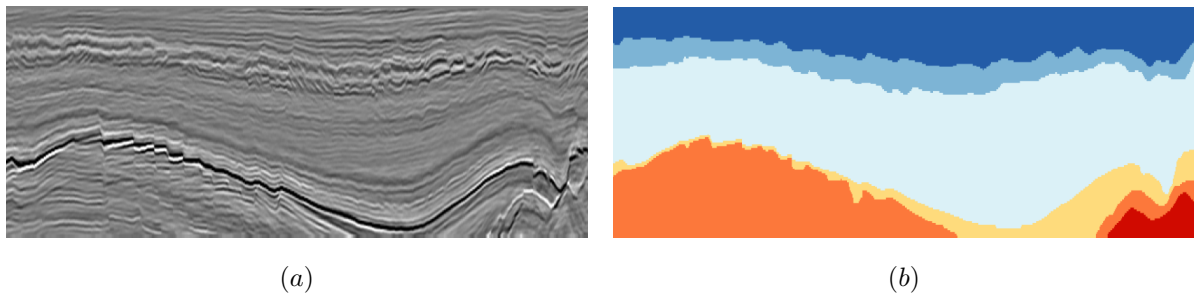


Figure 2. Data contained in the Dataset. In (a) an inline section and in (b) its corresponding label.

Table 1. The percentage of pixels for each class in the training set.

Zechstein	Scruff	Rijnland/Clak	Lower N. S.	Middle N. S.	Upper N. S.
1.48%	3.21%	6.62%	48.43%	11.84%	28.43%

3.2 Attribute extraction and Aggregation

We used the OpenTect [9] software version 6.6 to extract the seismic attributes from the amplitude data contained in the Dataset. An expert chose the attributes: Instantaneous Phase, Texture, Energy, and Pseudo Relief, as they have relevant characteristics and represent the seismic in a well attenuated way, as well as the amplitude data. We generated a volume for each attribute, the same size as the original amplitude data, and then they were divided into three blocks, one for training and the others for testing. Thus, as the amplitude data contained in the Dataset, which the authors divided into three blocks.

The attributes were grouped, after extraction, forming a kind of channel each. For example, given an inline referring to the amplitude data, it contained the other inlines of each attribute respectively coupled. In the end, this inline would have a kind of five channels, one for amplitude, and another four of the attributes. Thus, it was done for all inlines and crosslines used in this work. We did experiments without the amplitude data, in this case, only the attributes were grouped, as mentioned above. Figure 3 presents an example in an inline of how the grouping and its entry in the network were.

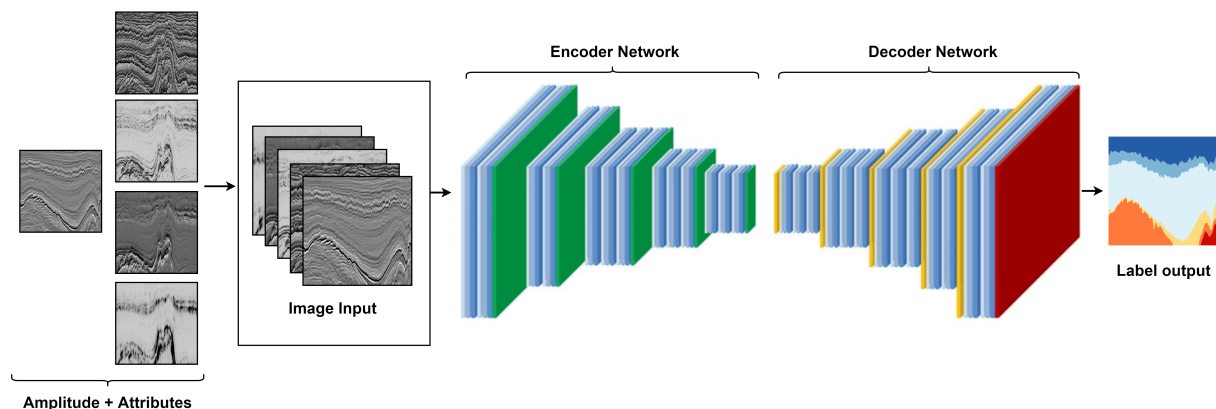


Figure 3. Example network input image.

3.3 Architecture and Loss function

After the attributes were selected and prepared, we used an open source network available by [5] to perform the classification of the seismic layers. It is an architecture based on VGG16 modified to have batch normalization. The network consists of two parts, an encoder, and a decoder. The encoder part of the network corresponds to a feature extractor that transforms the input data into a multidimensional representation of features. The decoder part of the model represents a shape generator that provides the segmentation for the input classes from the features

retrieved from the encoder. Finally, the output layer shows the probability that each pixel belongs to one of the predetermined classes with the same size as the input data.

Figure 4 shows the network architecture used. The white layers on the encoder side are convolution, and the decoder side is deconvolution, the red layers are max-pooling, and the green layers are unpooling. Each convolution or deconvolution layer is followed by a rectified linear unit (ReLU). Layers in red perform 2 x 2 max-pooling to select maximum filter response in small windows. The indices of the maximum responses for each pooling layer are then shared with their respective unpooling layers to undo this pooling operation and obtain a higher resolution image [5].

We added more channels in the seismic data, so the network input had to be adapted to accept this new modified data, becoming a multichannel architecture.

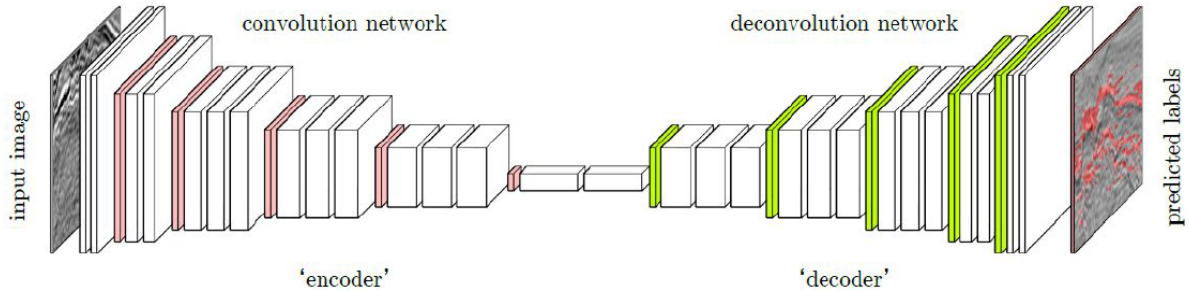


Figure 4. Deconvolution network architecture. Fonte: Alaudah et al. [5]

The loss function used was the Weighted cross-entropy (WCE) [10] to solve the problem of class imbalance in the dataset. Classes with few sample numbers do not contribute significantly to the total loss and tend to be ignored during training. One way to remedy this problem is to assign proper weights to each class. The equation is defined as:

$$WCE = -\frac{1}{N} \sum_{n=1} w r_n \log(p_n) + (1 - r_n) \log(1 - p_n), \quad (1)$$

where w is a weight vector whose value can be chosen by the user class by class and fixed or automatically adjusted during training, a higher value of w increases the importance of the specified class during training. r_n represents the reference value, p_n is the predicted value, and N is the total samples.

3.4 Evaluation Metrics

To evaluate the performance of the model, we used a set of metrics based on [5] which the following: Accuracy per pixel (2), which is the percentage of pixels over all classes that are classified correctly, accuracy per class (3), represents the percentage of pixels that are correctly classified of a class, the average of the accuracy per class (4), which is the sum of the accuracy per class divided by the total of classes, and the Frequency Weighted Intersection over Union (5) which is a metric based on the Intersection over Union only weighted, to evaluate classes unbalanced better. The equations are defined as:

$$PA = \frac{\sum_i |F_i \cap G_i|}{\sum_i |G_i|} \quad (2)$$

$$CA_i = \frac{|F_i \cap G_i|}{|G_i|} \quad (3)$$

$$MCA = \frac{1}{n_c} \sum_i \frac{|F_i \cap G_i|}{|G_i|} \quad (4)$$

$$FWIU = \frac{1}{\sum_i |G_i|} \cdot \sum_i |G_i| \cdot \frac{|F_i \cup G_i|}{|F_i \cap G_i|} \tag{5}$$

Where G_i is the set of pixels that belong to the class i , and F_i is the set of pixels classified as class i . Thus, the set of correctly classified pixels is $F_i \cap G_i$. Moreover, N_c is the number of classes.

4 Experiments and Results

Sections of inlines and crosslines were used in the training set, totaling 1102 samples, 10% being separated for validation. Because they are different sizes, the dimensions of the sections have been resized to 256×256 to avoid scaling issues with the network.

Two test scenarios were defined, the first one with the attributes grouped together, and the second with the attributes plus amplitude grouped. The training settings used are defined in Table 2. All experiments were performed three times and averaged. After training the network, the metrics discussed in the 3.4 section were calculated. Then, a post-processing step was carried out, where a resampling was performed to obtain the original size of the images, in the same way that it was done for training, but in reverse.

Table 2. Network training settings.

Epochs	500 with Early Stopping
Learning rate	0.001
Optimizer	Adam
Batch size	8

The results obtained in scenarios 1 and 2 are presented in Table 3. It also shows the comparison with a related work mentioned in section 1 on which our work is strongly inspired. The amplitude, which is the most commonly used data for the seismic classification task, obtained 81.23%, scenario 1, which is the attributes together, obtained 85.15%, and scenario 2, which is the attributes and the amplitude together, reached 85.73%, based on the FWIU metric.

Table 3. Result of evaluation metrics for test scenarios.

	PA	Class Accuracy						MCA	FWIU
		Zechstein	Scruff	Rijnland/Clak	Lower N. S.	Middle N. S.	Upper N. S.		
Amplitude	0.890	0.425	0.517	0.735	0.963	0.892	0.971	0.751	0.812
Attributes	0.911	0.563	0.631	0.710	0.977	0.903	0.973	0.793	0.851
Att + Amp	0.912	0.618	0.595	0.737	0.981	0.898	0.976	0.801	0.857
Alaudah et al. [5]	0.905	0.602	0.674	0.772	0.941	0.938	0.974	0.817	0.832

We can see that the attributes obtained a better result in all metrics compared to the amplitude result, that is, combining several attributes in a single classification process proved to be quite effective.

Comparing our work with Alaudah et al. [5], the best result they obtained was using data augmentation, they achieved 83.20% while ours, even not using this technique, obtained a better result reaching 85.70% based on the FWIU metric. Thus, comparing the model with data augmentation and a model with attributes, the multiattribute performed better.

Figure 5 shows a case of model success in the test dataset. In it, we have an inline that contains the six layers, observing the prediction, the network got practically all right, containing only minor errors, but in general, the prediction was very satisfactory.

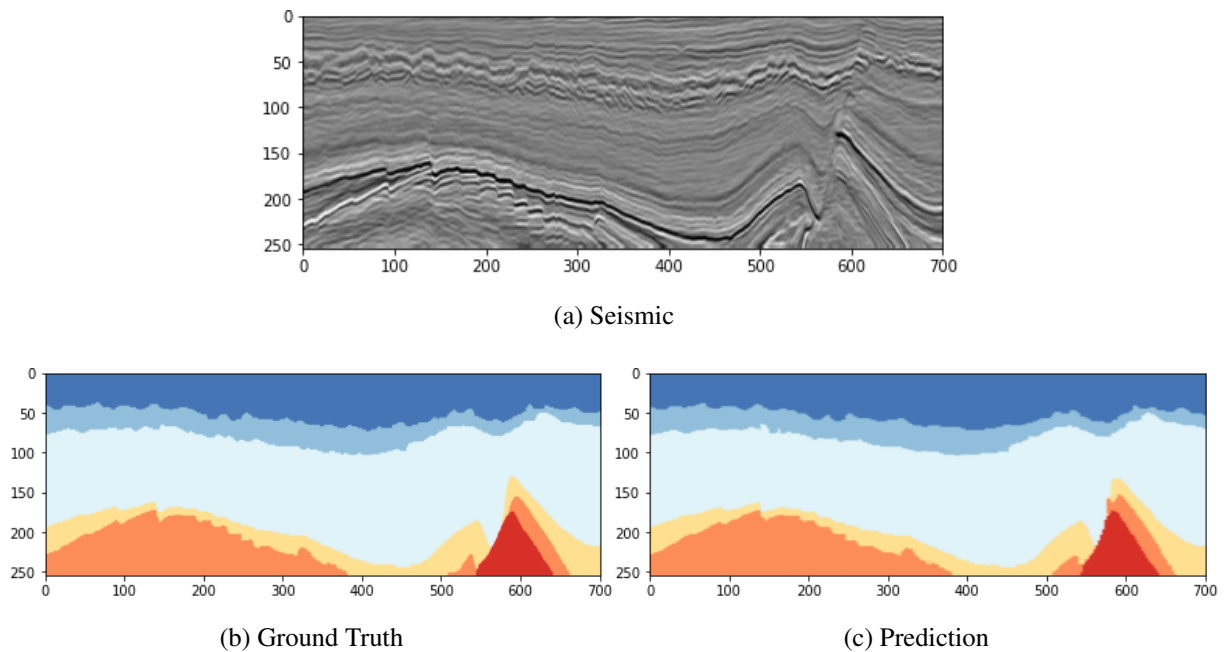


Figure 5. Hit case in one inline from test set 1.

Figure 6 presents a case of model error. We can see that the prediction of the network was wrong in three of the six classes they had in the inline, the errors were in the three minority classes (red, orange, and yellow). These errors are due to the unbalanced dataset, and the network has difficulty getting the smaller classes right, as they contain less information about them.

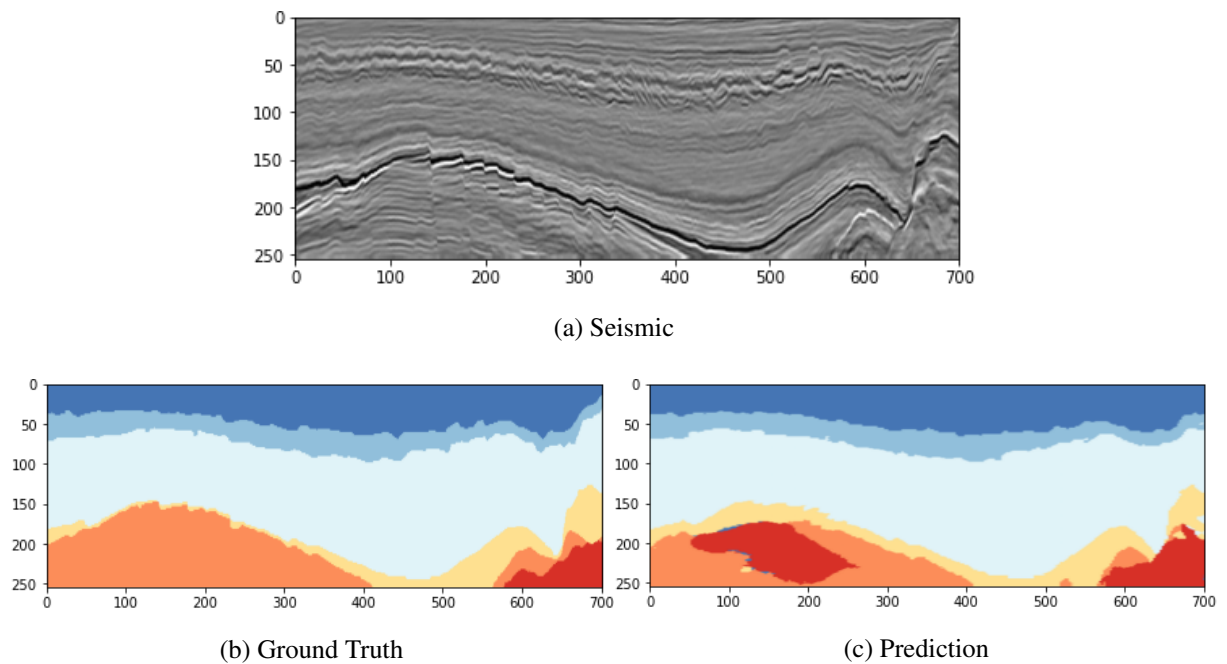


Figure 6. Error case in one inline from test set 1.

5 Conclusions and Future Works

The present work presents a methodology for classifying seismic facies in seismic data. A set of actual open data was used and compared directly with Alaudah et al. [5] work, to validate the method. Quantitative metrics and model predictions confirm the quality of the results. The method uses the combination of a set of seismic attributes and the amplitude to classify the seismic facies of the seismic data. For this, an encoder-decoder network was used for multiple data inputs. As the seismic layers were considerably unbalanced, the Binary Cross entropy

loss function was used to overcome this problem.

The best result obtained was using the attributes grouped with the amplitude in a single classification process, reaching 85.73%, based on the FWIU metric. The results also showed that using multi-attributes in this classification problem task performed better than the model with data augmentation.

Finally, this work presented a new approach for the seismic facies classification problem using multi-attributes. For future work, it would be interesting to put a mechanism in the input for automatic selection of attributes instead of manual selection. As well as testing other combinations of them.

Acknowledgements. The present work was carried out with the support of the Tecgraf Institute and the CNPq (National Council for Scientific and Technological Development).

Authorship statement. The authors hereby confirm that they are the sole liable persons responsible for the authorship of this work, and that all material that has been herein included as part of the present paper is either the property (and authorship) of the authors, or has the permission of the owners to be included here.

References

- [1] P. H. L. Fontes and S. Bahia. O uso de atributos sísmicos na delimitação da rocha geradora da região do baixo de miranga-bacia do recôncavo. Monography, Universidade Federal da Bahia, Salvador, BA, 2018.
- [2] T. Randen, E. Monsen, C. Signer, A. Abrahamsen, J. O. Hansen, T. Sæter, and J. Schlaf. Three-dimensional texture attributes for seismic data analysis. In *SEG Technical Program Expanded Abstracts 2000*, pp. 668–671. Society of Exploration Geophysicists, 2000.
- [3] S. Chopra and K. J. Marfurt. Seismic attributes—a historical perspective. *Geophysics*, vol. 70, n. 5, pp. 3SO–28SO, 2005.
- [4] M. Liu, M. Jervis, W. Li, and P. Nivlet. Seismic facies classification using supervised convolutional neural networks and semisupervised generative adversarial networks. *Geophysics*, vol. 85, n. 4, pp. O47–O58, 2020.
- [5] Y. Alaudah, P. Michałowicz, M. Alfarraj, and G. AlRegib. A machine-learning benchmark for facies classification. *Interpretation*, vol. 7, n. 3, pp. SE175–SE187, 2019.
- [6] F. Li, H. Zhou, Z. Wang, and X. Wu. Addcnn: An attention-based deep dilated convolutional neural network for seismic facies analysis with interpretable spatial–spectral maps. *IEEE Transactions on Geoscience and Remote Sensing*, vol. 59, n. 2, pp. 1733–1744, 2020.
- [7] J. El Zini, Y. Rizk, and M. Awad. A deep transfer learning framework for seismic data analysis: A case study on bright spot detection. *IEEE Transactions on Geoscience and Remote Sensing*, vol. 58, n. 5, pp. 3202–3212, 2020.
- [8] H. Zhang, T. Chen, Y. Liu, Y. Zhang, and J. Liu. Automatic seismic facies interpretation using supervised deep learning. *Geophysics*, vol. 86, n. 1, pp. IM15–IM33, 2021.
- [9] G. E. Sciences. Gb earth sciences, opendtect. <https://www.dgbes.com/index.php/software/free#opendtect>. Acessado: 13-12-2021, 2018.
- [10] C. H. Sudre, W. Li, T. Vercauteren, S. Ourselin, and M. Jorge Cardoso. Generalised dice overlap as a deep learning loss function for highly unbalanced segmentations. In *Deep learning in medical image analysis and multimodal learning for clinical decision support*, pp. 240–248. Springer, 2017.